ERRORS DUE TO THE COMMON RAY APPROXIMATIONS OF THE COUPLING RAY THEORY

L. Klimeš and P. Bulant

Department of Geophysics, Faculty of Mathematics and Physics, Charles University,
Ke Karlovu 3, 121 16 Praha 2, Czech Republic
(klimes@seis.karlov.mff.cuni.cz, bulant@seis.karlov.mff.cuni.cz)

Received: April 30, 2003; Revised: December 1, 2003; Accepted: January 5, 2004

ABSTRACT

The common ray approximation considerably simplifies the numerical algorithm of the coupling ray theory for S waves, but may introduce errors in travel times due to the perturbation from the common reference ray. These travel–time errors can deteriorate the coupling–ray–theory solution at high frequencies. It is thus of principal importance for numerical applications to estimate the errors due to the common ray approximation.

We derive the equations for estimating the travel–time errors due to the isotropic and anisotropic common ray approximations of the coupling ray theory. These equations represent the main result of the paper. The derivation is based on the general equations for the second–order perturbations of travel time. The accuracy of the anisotropic common ray approximation can be studied along the isotropic common rays, without tracing the anisotropic common rays.

The derived equations are numerically tested in three 1-D models of differing degree of anisotropy. The first–order and second–order perturbation expansions of travel time from the isotropic common rays to anisotropic–ray–theory rays are compared with the anisotropic–ray–theory travel times. The errors due to the isotropic common ray approximation and due to the anisotropic common ray approximation are estimated. In the numerical example, the errors of the anisotropic common ray approximation are considerably smaller than the errors of the isotropic common ray approximation.

The effect of the isotropic common ray approximation on the coupling–ray–theory synthetic seismograms is demonstrated graphically. For comparison, the effects of the quasi–isotropic projection of the Green tensor, of the quasi–isotropic approximation of the Christoffel matrix, and of the quasi–isotropic perturbation of travel times on the coupling–ray–theory synthetic seismograms are also shown. The projection of the travel–time errors on the relative errors of the time–harmonic Green tensor is briefly presented.

Keywords: coupling ray theory, common ray approximation, travel time, perturbation theory, seismic anisotropy, inhomogeneous media

1. INTRODUCTION

In the isotropic ray theory, the S–wave polarization vectors do not rotate about the ray, whereas in the anisotropic ray theory they coincide with the eigenvectors of the Christoffel matrix which may rotate rapidly about the ray. In "weakly anisotropic" models, at moderate frequencies, the S–wave polarization tends to remain unrotated round the ray but is partly attracted by the rotation of the eigenvectors of the Christoffel matrix. The intensity of the attraction increases with frequency. This behaviour of the S–wave polarization is described by the *coupling ray theory* proposed by *Coates and Chapman (1990)*. The coupling ray theory is applicable to S waves at all degrees of anisotropy, from isotropic models to considerably anisotropic ones. The numerical algorithm for calculating the frequency–dependent complex–valued S–wave polarization vectors of the coupling ray theory has been designed by *Bulant and Klimeš (2002)*.

There are many commonly used *quasi–isotropic approximations* of the coupling ray theory (*Pšenčík, 1998a*), which diminish the accuracy of the coupling ray theory both with increasing frequency and increasing degree of anisotropy. Most of these quasi–isotropic approximations can be avoided with minimal effort (*Bulant and Klimeš, 2002; 2004*), except for the *common ray approximation* for S waves. In the common ray approximation, only one reference ray is traced for both anisotropic–ray-theory S waves, and both S–wave anisotropic–ray-theory travel times are approximated by the perturbation expansion from the common reference ray. The common ray approximation thus considerably simplifies the coding of the coupling ray theory and numerical calculations, but may introduce errors in travel times due to the perturbation. These travel–time errors can deteriorate the coupling–ray–theory solution at high frequencies. It is thus of principal importance for numerical applications to estimate the travel–time errors due to the common ray approximation, and then the related error of the wavefield.

In the common ray approximation, the S–wave travel times are usually approximated by the first–order perturbation expansion from the common reference ray. The errors of S–wave travel times may then be approximated by second–order terms in the perturbation expansion. The calculation of these estimates of travel–time errors due to the *isotropic common ray approximation* and the *anisotropic common ray approximation* (*Bakker, 2002*; *Klimeš, 2003*) is proposed and numerically demonstrated in this paper. The equations for estimating the travel–time errors due to the isotropic and anisotropic common ray approximations of the coupling ray theory for S waves are derived in a form suitable for dynamic ray tracing in ray–centred (Riemannian normal) coordinates.

Note that the perturbation expansion is the Taylor expansion with respect to the perturbation parameters, see (17), which parametrize the Hamiltonian, see (16). We refer here to the partial derivatives with respect to the perturbation parameters as perturbation derivatives, in order to distinguish them from the partial derivatives with respect to the spatial coordinates.

2. COMMON RAY APPROXIMATIONS

For the derivation of the coupling ray theory refer to *Coates and Chapman (1990)* and *Červený (2001)*. For the description of the numerical algorithm refer to *Červený (2001)* and *Bulant and Klimeš (2002)*. Here we shall concentrate only on estimating the travel–time errors due to the common ray approximations. The estimates are based on the equations for the second–order perturbation derivatives of travel time derived by *Klimeš (2002)*.

2.1. Selection of the reference ray

The isotropic ray theory is always the limiting case of the coupling ray theory for decreasing anisotropy at a fixed frequency. On the other hand, the high–frequency limit of the coupling ray theory at a fixed anisotropy depends on the choice of the reference ray, and even on the choice of the *system* of reference rays, because the amplitudes are determined by the paraxial reference rays. The reference ray should be "close to the ray of the coupled S wave under study". Unfortunately, this is nothing but a rough statement, because the ray of the coupled S wave has not been defined yet.

From the point of view of the high–frequency asymptotic validity, the frequency–independent reference ray is best represented by the *anisotropic–ray–theory reference ray*, provided we choose the initial condition for the polarization vector in the coupling equation given by the eigenvector of the Christoffel matrix corresponding to the reference ray. The anisotropic–ray–theory travel time corresponding to the selected polarization is then exact, and only the difference between the two anisotropic–ray–theory S–wave travel times is approximate. The coupling ray theory may then also be used at high frequencies because the approximate travel–time difference influences only the coupling due to low–frequency scattering. The coupling ray theory then correctly converges to the anisotropic ray theory for high frequencies. For other choices of reference rays, the high–frequency limit of the coupling ray theory at a fixed anisotropy is incorrect, although the differences may be small at the finite frequencies under consideration. Note that the anisotropic–ray–theory reference ray can be traced only if the eigenvectors of the Christoffel matrix vary continuously along the whole ray (*Vavryčuk, 2001*).

In the *anisotropic common ray approximation*, the common reference ray is traced using the averaged Hamiltonian of both anisotropic–ray-theory S waves (*Bakker, 2002*; *Klimeš, 2003*).

In the less accurate *isotropic common ray approximation*, the reference ray is traced in the reference isotropic model. Moreover, the reference isotropic model may be selected in different ways, yielding quasi–isotropic approximations of differing accuracies.

2.2. First–order perturbation expansion of travel time

Let $a_{ijkl} = a_{ijkl}(x_m)$ be the density–normalized elastic moduli describing a *smooth anisotropic model*, and $v_0 = v_0(x_m)$ the S–wave velocity in the smooth *reference isotropic model* used to trace the "isotropic" reference rays. We shall refer to v_0 briefly as the reference velocity.

Assume a phase–space *reference ray*, parametrized by reference travel time τ, with reference slowness vectors $p_i(\tau)$ known at all its points $x_j(\tau)$. Using the reference slowness vectors, we can calculate reference Christoffel matrix

$$\Gamma_{jk}(\tau) = p_i(\tau)\, a_{ijkl}(x_m(\tau))\, p_l(\tau) \tag{1}$$

and its eigenvectors $g_{i\alpha}(\tau)$, $\alpha = 1, 2, 3$ along the reference ray. Whereas the Einstein summation over the pairs of identical Roman indices (both subscripts and superscripts) $i, j, k, ... = 1, 2, 3$ or $I, J, K, ... = 1, 2$ is used throughout this paper, no implicit summation applies to Greek subscripts $\alpha, \beta, ...$ indexing the eigenvectors of the Christoffel matrix. Assume that eigenvectors $g_{i1}(\tau)$ and $g_{i2}(\tau)$ correspond to the S waves, and eigenvector $g_{i3}(\tau)$ to the P wave. For application of the coupling ray theory, the eigenvectors should vary continuously along the reference ray (*Bulant and Klimeš, 2002*). This condition is not required in regions where the two S–wave eigenvalues of the Christoffel matrix are approximately equal.

Let us denote by $\tau_\alpha(\tau)$ the anisotropic–ray-theory travel time corresponding to the selected eigenvector $g_{i\alpha}(\tau)$ of the Christoffel matrix. It may be approximated by a quadrature along the unperturbed reference ray,

$$\frac{\mathrm{d}\tau_\alpha}{\mathrm{d}\tau} = [\Gamma_{jk} g_{j\alpha} g_{k\alpha}]^{-\frac{1}{2}} \quad . \tag{2}$$

Travel–time approximation (2), suggested for the coupling ray theory by *Bulant and Klimeš (2002)*, would become exact for a reference ray following the path of the exact ray. Travel–time approximation (2) can be derived as the first–order part of perturbation expansion (17), corresponding to Hamiltonian

$$H_\alpha(x_m, p_n) = -[G_\alpha(x_m, p_n)]^{-\frac{1}{2}} \quad , \tag{3}$$

where $G_\alpha(x_m, p_n)$ is the eigenvalue of Christoffel matrix (1), corresponding to eigenvector $g_{i\alpha}$ (*Klimeš, 2002,* eqs. 43 and 65).

2.3. Reference isotropic Hamiltonian and correct anisotropic Hamiltonians

Hamiltonian (3), specified for the reference isotropic medium, is given by

$$H_0(x_m, p_n) = -[v_0(x_m)]^{-1}(p_i p_i)^{-\frac{1}{2}} \quad . \tag{4}$$

The value of Hamiltonian (4) at the reference ray is

$$H_0 = -1 \quad . \tag{5}$$

The partial derivatives with respect to spatial coordinates x_i, denoted by Roman subscripts following a comma, of Hamiltonian (4) are

$$H_{0,i} = v_{0,i}\,(v_0)^{-2}(p_i p_i)^{-\frac{1}{2}} \quad , \tag{6}$$

which is, at the reference ray, equal to

$$\boxed{H_{0,i} = v_{0,i}\,(v_0)^{-1} \quad .} \tag{7}$$

The partial derivatives with respect to the components of the slowness vector, denoted by Roman superscripts following a comma, of Hamiltonian (4) are

$$H_0^{;i} = (v_0)^{-1}(p_k p_k)^{-\frac{3}{2}} p_i \quad , \tag{8}$$

which is, at the reference ray, equal to

$$H_0^{;i} = (v_0)^2 p_i \quad . \tag{9}$$

The second–order partial derivatives of Hamiltonian (4) with respect to the components of the slowness vector are

$$H_0^{;ij} = (v_0)^{-1}(p_k p_k)^{-\frac{3}{2}}\, \delta^{ij} - 3\,(v_0)^{-1}(p_k p_k)^{-\frac{5}{2}}\, p_i p_j \quad , \tag{10}$$

which is, at the reference ray, equal to

$$H_0^{;ij} = (v_0)^2\, \delta^{ij} - 3\,(v_0)^4\, p_i p_j \quad . \tag{11}$$

Kronecker symbol δ^{ij} denotes the components of the identity matrix.

The value of Hamiltonian (3), corresponding to unit eigenvector $g_{i\alpha}$ of the Christoffel matrix, at the reference ray, is

$$\boxed{H_\alpha = -(a_{ijkl} g_{i\alpha} p_j g_{k\alpha} p_l)^{-\frac{1}{2}} \quad .} \tag{12}$$

The partial derivatives of Hamiltonian (12) with respect to the spatial coordinates are

$$\boxed{H_{\alpha,i} = -\tfrac{1}{2}(H_\alpha)^3 a_{mjkl,i} g_{m\alpha} p_j g_{k\alpha} p_l \quad .} \tag{13}$$

The partial derivatives of Hamiltonian (12) with respect to the components of the slowness vector are

$$\boxed{H_\alpha^{;i} = -(H_\alpha)^3 a_{mikl} g_{m\alpha} g_{k\alpha} p_l \quad .} \tag{14}$$

The values of phase–space derivatives (13) and (14) are calculated at the reference ray in this paper. Partial derivatives (14) satisfy Euler's relation

$$H_\alpha^{;i} p_i = -H_\alpha \tag{15}$$

for a homogeneous function of degree -1 with respect to p_i.

The quantities enclosed above in boxes are necessary for estimating the errors due to the common ray approximations of the coupling ray theory.

2.4. Parametric system of the Hamiltonians and errors due to the common ray approximations

We consider the two–parametric set $H = H(x_m, p_n, f_\alpha)$ of Hamiltonians parametrized by f_α, $\alpha = 1, 2$ for an S wave, or the one–parametric set $H = H(x_m, p_n, f_\alpha)$ of Hamiltonians parametrized by f_α, $\alpha = 3$ for a P wave,

$$H(x_m, p_n, f_\alpha) = H_0(x_m, p_n) + \sum_\alpha [H_\alpha(x_m, p_n) - H_0(x_m, p_n)]\, f_\alpha \quad . \tag{16}$$

Parameters f_α are called *perturbation parameters* (*Baumgärtel, 1985*) or model parameters (*Tarantola, 1987*; *Klimeš, 2002*). Parametric system (16) of the Hamiltonians then generates parametric system $\tau(x_m, f_\alpha)$ of the travel–time fields corresponding to the individual Hamiltonians $H(x_m, p_n, f_\alpha)$.

For an S wave, we obtain the Hamiltonian corresponding to the isotropic common ray approximation in the reference isotropic model for $(f_1, f_2) = (0, 0)$, the Hamiltonian corresponding to the first anisotropic–ray-theory S wave for $(f_1, f_2) = (1, 0)$, the Hamiltonian corresponding to the second anisotropic–ray-theory S wave for $(f_1, f_2) = (0, 1)$, and the averaged Hamiltonian of both anisotropic–ray-theory S waves corresponding to the anisotropic common ray approximation by *Bakker (2002)* for $(f_1, f_2) = (\frac{1}{2}, \frac{1}{2})$.

For a P wave, we obtain the Hamiltonian corresponding to the reference ray in the reference isotropic model for $f_3 = 0$, and the Hamiltonian corresponding to the anisotropic P wave for $f_3 = 1$.

The Taylor expansion with respect to perturbation parameters f_α is called *perturbation expansion.* The second–order perturbation expansion of travel time is

$$\tau(x_m, f_\alpha) \approx \tau(x_m) + \sum_\alpha \tau_{,\alpha}(x_m) f_\alpha + \tfrac{1}{2} \sum_\alpha \sum_\beta \tau_{,\alpha\beta}(x_m) f_\alpha f_\beta \quad , \tag{17}$$

where the Greek subscripts following a comma denote the partial derivatives with respect to perturbation parameters f_α, called hereinafter the *perturbation derivatives.* Note that *Klimeš (2002)* refers to the perturbation derivatives briefly as the "perturbations". Here, travel time $\tau(x_m)$ and its perturbation derivatives $\tau_{,\alpha}(x_m)$, $\tau_{,\alpha\beta}(x_m)$, with arguments f_α omitted, correspond to the reference model $f_\alpha = 0$.

Travel–time approximation (2) corresponds to the first–order part of perturbation expansion (17). The error of travel–time approximation (2) may thus be approximated by the quadratic term in perturbation expansion (17).

We may now express the estimates of the travel–time errors due to the *isotropic common ray* (ICR) *approximation* of anisotropic travel times in terms of the second–order perturbation derivatives of travel time. The errors of travel–time approximation (2) from isotropic common reference ray $(f_1, f_2) = (0, 0)$ to the correct anisotropic S–wave ray $(f_1, f_2) = (1, 0)$ and to the correct anisotropic S–wave ray $(f_1, f_2) = (0, 1)$ are approximately

$$\boxed{\delta\tau_\alpha^{\mathrm{ICR}} = \frac{\tau_{,\alpha\alpha}}{2} \quad , \qquad (18)}$$

where $\alpha = 1, 2$ for S waves. Equation (18) with $\alpha = 3$ analogously yields the estimate of the error of travel–time approximation (2) from isotropic reference P–wave ray $f_3 = 0$ to the correct anisotropic P–wave ray $f_3 = 1$.

We may also use the second–order perturbation derivatives of travel time, calculated along the isotropic common reference ray, to estimate the accuracy of the *anisotropic common ray* (ACR) *approximation* (*Bakker, 2002*; *Klimeš, 2003*). The estimates of errors of travel–time approximation (2) from the anisotropic common S–wave reference ray $(f_1, f_2) = (\frac{1}{2}, \frac{1}{2})$ to $(f_1, f_2) = (1, 0)$ and to $(f_1, f_2) = (0, 1)$ are equal,

$$\boxed{\delta\tau_\alpha^{\mathrm{ACR}} = \frac{\tau_{,11} - 2\tau_{,12} + \tau_{,22}}{8} \quad , \qquad (19)}$$

where $\alpha = 1, 2$. Error estimates (19) represent the contributions of the quadratic terms in perturbation expansion (17) at the distances from the anisotropic common S–wave reference ray to the correct S–wave rays.

To calculate the first–order and second–order perturbation derivatives $\tau_{,\alpha}$ and $\tau_{,\alpha\beta}$ of travel time, we need the first–order and second–order phase–space and perturbation derivatives of the Hamiltonian. The phase–space and perturbation derivatives of Hamiltonian (16) in the reference model $f_\alpha = 0$ are

$$H_{,i} = H_{0,i} \quad , \tag{20}$$

$$H^{,i} = H_0^{,i} \quad , \tag{21}$$

$$H^{,ij} = H_0^{,ij} \quad , \tag{22}$$

$$H_{,\alpha} = H_\alpha - H_0 \quad , \tag{23}$$

$$H_{,i\alpha} = H_{\alpha,i} - H_{0,i} \quad , \tag{24}$$

$$H^{,i}_{,\alpha} = H_\alpha^{,i} - H_0^{,i} \quad , \tag{25}$$

$$H_{,\alpha\beta} = 0 \quad , \tag{26}$$

where the Greek subscripts following a comma denote the partial derivatives with respect to perturbation parameters f_α, analogously as for travel time.

2.5. Dynamic ray tracing and ray–centred coordinates

We define the matrices of the partial derivatives of spatial coordinates x_i and of the slowness–vector components $p_i = \tau_{,i}$ with respect to 3 *ray coordinates*: ray take–off parameters γ_1, γ_2, and independent parameter $\gamma_3 = \tau$ along rays,

$$Q_{ia} = \frac{\partial x_i}{\partial \gamma_a} \quad , \qquad P_{ia} = \frac{\partial \tau_{,i}}{\partial \gamma_a} \quad . \tag{27}$$

Matrices Q_{ia} and P_{ia} can be calculated by numerically solving a set of linear ordinary differential equations called the *dynamic ray tracing equations* (*Babich and Buldyrev, 1972*; *Červený, 1972*; *Arnaud, 1973*; *Červený and Hron, 1980*). Matrices Q_{ia}

and P_{ia} describe, by definition, the properties of the orthonomic system of rays corresponding to the travel time under consideration. They may be expressed in terms of their initial values and the paraxial ray propagator matrix (*Červený, 2001*).

The second-order spatial derivatives $\tau_{,ij}$ of travel time can be expressed in terms of matrices Q_{ia} and P_{ia}. Equation

$$P_{ia} = \tau_{,ij}\, Q_{ja} \tag{28}$$

is a direct consequence of the above definitions (27).

Let us denote by h_{i1}, h_{i2}, h_{i3} the basis vectors of the *ray-centred coordinate system* (Riemannian normal coordinate system) proposed by *Luneburg (1944)*, *Babich and Buldyrev (1972)* and *Popov and Pšenčík (1978a; 1978b)*. The orthonormal basis vectors of the ray-centred coordinate system are calculated along the reference ray in the reference isotropic model. The first two basis vectors h_{iM} of the ray-centred coordinate system are tangent to the wavefront, the third basis vector $h_{i3} = v_0 p_i$ is tangent to the ray. The equations for calculating the basis vectors of the ray-centred coordinate system can be found, e.g., in the book by *Červený (2001)*.

The quantities covariantly transformed from spatial coordinates x_i to the local Cartesian basis h_{im} of the ray-centred coordinate system are marked by a tilde $\tilde{}$. In particular,

$$\widetilde{Q}_{ia} = h_{mi} Q_{ma} \quad , \tag{29}$$

$$\widetilde{P}_{ia} = h_{mi} P_{ma} \quad , \tag{30}$$

$$\widetilde{\tau}_{,ij} = h_{mi} \tau_{,mn} h_{nj} \quad , \tag{31}$$

$$\widetilde{\tau}_{,i\alpha} = h_{mi} \tau_{,m\alpha} \quad , \tag{32}$$

$$\boxed{\begin{aligned} \widetilde{H}_{0,i} &= H_{0,m} h_{mi} \quad , & (33) \\ \widetilde{H}_{\alpha,i} &= H_{\alpha,m} h_{mi} \quad , & (34) \\ \widetilde{H}_{\alpha}^{\,i} &= H_{\alpha}^{\,m} h_{mi} \quad . & (35) \end{aligned}}$$

Since we consider matrices Q_{ia} and P_{ia} defined for $\gamma_3 = \tau$,

$$\widetilde{Q}_{3J} = 0 \quad . \tag{36}$$

The 2×2 submatrices $\widetilde{Q}_{IJ}$ and $\widetilde{P}_{IJ}$ of matrices (29) and (30) are usually calculated by the *dynamic ray tracing equations in ray-centred coordinates (Červený, 2001,* eq. 4.1.65),

$$\frac{\mathrm{d}}{\mathrm{d}\tau} \widetilde{Q}_{IJ} = (v_0)^2\, \widetilde{P}_{IJ} \quad , \tag{37}$$

$$\frac{\mathrm{d}}{\mathrm{d}\tau} \widetilde{P}_{IJ} = -(v_0)^{-1} \widetilde{(v_0)}_{,IK} \widetilde{Q}_{KJ} \quad , \tag{38}$$

where

$$\widetilde{(v_0)}_{,IK} = h_{mI}\, (v_0)_{,mn}\, h_{nJ} \tag{39}$$

are the second-order spatial derivatives of the velocity in ray-centred coordinates.

We shall thus express the equations for estimating the travel-time errors due to the common ray approximations of the coupling ray theory in terms of the 2×2 matrices $\widetilde{Q}_{IJ}$ and $\widetilde{P}_{IJ}$ in ray-centred coordinates.

2.6. First–order perturbation derivatives of the travel–time gradient

To calculate the second–order perturbation derivatives of travel time, we need to know at least the ray–normal projection

$$\tau^{\perp}_{,i\alpha} = E^{\perp}_{ij}\tau_{,j\alpha} \tag{40}$$

of the first–order perturbation derivatives $\tau_{,i\alpha}$ of the travel–time gradient (*Klimeš, 2002,* eqs. 54 and 55). The ray–normal projection matrix $E^{\perp}_{ij}$ can be expressed in terms of the first two basis vectors of the ray–centred coordinate system,

$$E^{\perp}_{ij} = h_{iM}h_{jM} \quad . \tag{41}$$

The covariant transform (*Klimeš, 2002,* eq. 69)

$$T^{\perp}_{J\alpha} = \tau^{\perp}_{,i\alpha}\, Q_{iJ} \tag{42}$$

of ray–normal derivatives (40) into ray coordinates can be determined by numerical quadrature (*Klimeš, 2002,* eq. 75)

$$\boxed{T^{\perp}_{J\alpha}(\tau) = T^{\perp}_{J\alpha}(\tau^0) + \int_{\tau^0}^{\tau} \mathrm{d}\tau\, K^{\perp}_{i\alpha} Q_{iJ}} \tag{43}$$

along the reference ray, with zero initial conditions $T^{\perp}_{J\alpha}(\tau^0) = 0$ at the point source.

The ray–normal integration kernel for the perturbation derivatives of the travel–time gradient is (*Klimeš, 2002,* eq. 80)

$$K^{\perp}_{i\alpha} = E^{\perp}_{ia}\,(-H_{,a\alpha} + H_{,a}\, H^{,r}_{,\alpha}\, p_r) - H^{,r}_{,\alpha}\, \tau^{\perp}_{,ri} \quad , \tag{44}$$

where

$$\tau^{\perp}_{,ij} = E^{\perp}_{ia}E^{\perp}_{jb}\tau_{,ab} \tag{45}$$

is the ray–normal projection of the second–order spatial derivatives $\tau_{,ij}$ of travel time.

Inserting equations (20), (24), (25) with (9) and (15), and (45) into (44), we arrive at

$$K^{\perp}_{i\alpha} = -E^{\perp}_{ia}\,(H_{\alpha,a} + H_{\alpha}H_{0,a}) - H^{,r}_{\alpha}\, E^{\perp}_{ra}\tau_{,ab}\, E^{\perp}_{bi} \quad . \tag{46}$$

Multiplying equation (46) by the first two columns Q_{iJ} of the matrix of geometrical spreading, inserting equation (41), and considering transforms (29), (30), (31) and relations (28) and (36), we arrive at

$$\boxed{K^{\perp}_{i\alpha}Q_{iJ} = -(\widetilde{H}_{\alpha,I} + H_{\alpha}\widetilde{H}_{0,I})\,\widetilde{Q}_{IJ} - \widetilde{H}^{,I}_{\alpha}\,\widetilde{P}_{IJ} \quad ,} \tag{47}$$

where $\widetilde{Q}_{IJ}$ and $\widetilde{P}_{IJ}$ are the 2×2 submatrices of matrices (29) and (30). The 2×2 matrices $\widetilde{Q}_{IJ}$ and $\widetilde{P}_{IJ}$ are usually calculated by the dynamic ray tracing equations (37) and (38) in ray–centred coordinates.

Inserting equations (40) and (41) into (42) while considering transforms (29) and (32), we arrive at

$$T^{\perp}_{J\alpha} = \widetilde{\tau}_{,I\alpha}\, \widetilde{Q}_{IJ} \quad . \tag{48}$$

The first–order perturbation derivatives of the travel–time gradient expressed in ray–centred coordinates are then

$$\widetilde{\tau}_{,I\alpha} = T^{\perp}_{J\alpha} \widetilde{Q}^{-1}_{JI} \quad , \tag{49}$$

where $\widetilde{Q}^{-1}_{JI}$ are the components of the matrix inverse to 2×2 matrix $\widetilde{Q}_{IJ}$ calculated by dynamic ray tracing (37) and (38) in ray–centred coordinates.

The value of $\widetilde{\tau}_{,I\alpha}$ at the point source, where $T^{\perp}_{J\alpha}(\tau^0) = 0$ and $\widetilde{Q}_{IJ}(\tau^0) = 0$, can be obtained by the l'Hospital rule with respect to $\tau \to \tau^0+$,

$$\widetilde{\tau}_{,I\alpha}(\tau^0) = -(v_0)^{-2} \widetilde{H}^{;I}_{\alpha} \quad . \tag{50}$$

2.7. Second–order perturbation derivatives of travel time

The second–order perturbation derivatives of travel time can be determined by numerical quadrature (*Klimeš, 2002,* eqs. 19 and 20)

$$\tau_{,\alpha\beta}(\tau) = \tau_{,\alpha\beta}(\tau^0) + \int_{\tau^0}^{\tau} \mathrm{d}\tau \ K_{\alpha\beta} \tag{51}$$

along the reference ray, with zero initial conditions $\tau_{,\alpha\beta}(\tau^0) = 0$ at the point source.

For Hamiltonian (3), the integration kernel for the second–order perturbation derivatives of travel time can be expressed as (*Klimeš, 2002,* eq. 64)

$$K_{\alpha\beta} = -H_{,\alpha\beta} - H^{;i}_{,\alpha} \tau^{\perp}_{,i\beta} - H^{;i}_{,\beta} \tau^{\perp}_{,i\alpha} - H^{;ij} \tau^{\perp}_{,i\alpha} \tau^{\perp}_{,j\beta} \quad . \tag{52}$$

Inserting relations (22) with (11), (25) with (9), and (26), equation (52) becomes

$$K_{\alpha\beta} = -H^{;i}_{\alpha} \tau^{\perp}_{,i\beta} - H^{;i}_{\beta} \tau^{\perp}_{,i\alpha} - (v_0)^2 \tau^{\perp}_{,i\alpha} \tau^{\perp}_{,i\beta} \quad . \tag{53}$$

Inserting relations (40) and (41), and considering transforms (32) and (35), equation (53) can be expressed in ray–centred coordinates as

$$K_{\alpha\beta} = -\widetilde{H}^{;I}_{\alpha} \widetilde{\tau}_{,I\beta} - \widetilde{H}^{;I}_{\beta} \widetilde{\tau}_{,I\alpha} - (v_0)^2 \widetilde{\tau}_{,I\alpha} \widetilde{\tau}_{,I\beta} \quad . \tag{54}$$

Equation (51) cannot be integrated numerically in the vicinities of caustics where $\widetilde{Q}_{IJ}$ is singular and $\widetilde{\tau}_{,I\alpha}$ in integration kernel (54) thus approach infinity. Fortunately, we may convert equation (51) analogously to *Klimeš (2002,* sec. 4.2*)*, but in ray–centred coordinates. Equation (51) with integration kernel (54) may be converted using dynamic ray tracing equations (37) and (38) and equation (43) with (47) into

$$\tau_{,\alpha\beta}(\tau) = \tau_{,\alpha\beta}(\tau^0) + \left[T^{\perp}_{I\alpha} \widetilde{Q}^{-1}_{IK} \widetilde{P}^{-1}_{JK} T^{\perp}_{J\beta} \right]^{\tau}_{\tau^0} + \int_{\tau^0}^{\tau} \mathrm{d}\tau \ K^{\mathrm{caust}}_{\alpha\beta} \tag{55}$$

with the modified integration kernel

$$\begin{aligned} K^{\mathrm{caust}}_{\alpha\beta} = & (\widetilde{H}_{\alpha,I} + H_{\alpha} \widetilde{H}_{0,I}) T^{\perp}_{J\beta} \widetilde{P}^{-1}_{JI} \\ & + (\widetilde{H}_{\beta,I} + H_{\beta} \widetilde{H}_{0,I}) T^{\perp}_{J\alpha} \widetilde{P}^{-1}_{JI} - (v_0)^{-1} \widetilde{(v_0)}_{,KL} T^{\perp}_{I\alpha} \widetilde{P}^{-1}_{IK} T^{\perp}_{J\beta} \widetilde{P}^{-1}_{JL} \quad . \end{aligned} \tag{56}$$

Combining equations (51) and (55) enables the optimization of calculating the second–order perturbation derivatives of travel time by numerical quadrature.

The second–order perturbation derivatives of travel time, calculated by quadratures (51) and (55), can be inserted into equation (18) for the travel–time errors due to the isotropic common ray approximation, and into equation (19) for the travel–time errors due to the anisotropic common ray approximation.

3. NUMERICAL EXAMPLE

The calculation of the first–order P–wave travel–time perturbation expansion from a reference isotropic model to an anisotropic model and the calculation of the S–wave coupling–ray–theory travel–time and amplitude corrections along the isotropic reference rays have been coded and added to the Fortran 77 package CRT (*Bucha and Bulant, 2002*). The package has been supplemented by the calculation of the second–order perturbation derivatives of travel times, which allows (a) estimation of the errors due to the isotropic common ray approximation of the coupling ray theory, (b) estimation of the errors due to the anisotropic common ray approximation of the coupling ray theory, and (c) approximate simulation of the results of the coupling ray theory with the anisotropic reference rays for testing purposes.

3.1. Model QI

A vertically heterogeneous 1-D anisotropic model QI was provided by *Pšenčík and Dellinger (2001,* model WA rotated by 45°*)* who performed the coupling–ray–theory calculations using the programs of package ANRAY (*Pšenčík, 1998b*) and compared the results with the reflectivity method. The density–normalized elastic moduli a_{ijkl} in km^{2}s^{-2} at the surface (zero depth) are

$$\begin{array}{c c} & \begin{array}{cccccc} 11 & 22 & 33 & 23 & 13 & 12 \end{array} \\ \begin{array}{c} 11 \\ 22 \\ 33 \\ 23 \\ 13 \\ 12 \end{array} & \begin{pmatrix} 14.48500 & 4.52500 & 4.75000 & 0.00000 & 0.00000 & -0.58000 \\ & 14.48500 & 4.75000 & 0.00000 & 0.00000 & -0.58000 \\ & & 15.71000 & 0.00000 & 0.00000 & -0.29000 \\ & & & 5.15500 & -0.17500 & 0.00000 \\ & & & & 5.15500 & 0.00000 \\ & & & & & 5.04500 \end{pmatrix} \end{array} , \qquad (57)$$

and at the depth of 1 km they are

$$\begin{array}{c c} & \begin{array}{cccccc} 11 & 22 & 33 & 23 & 13 & 12 \end{array} \\ \begin{array}{c} 11 \\ 22 \\ 33 \\ 23 \\ 13 \\ 12 \end{array} & \begin{pmatrix} 22.08963 & 6.90063 & 7.24375 & 0.00000 & 0.00000 & -0.88450 \\ & 22.08963 & 7.24375 & 0.00000 & 0.00000 & -0.88450 \\ & & 23.95775 & 0.00000 & 0.00000 & -0.44225 \\ & & & 7.86138 & -0.26688 & 0.00000 \\ & & & & 7.86138 & 0.00000 \\ & & & & & 7.69363 \end{pmatrix} \end{array} . \qquad (58)$$

Here the rows correspond to the first couple of indices of a_{ijkl}, the columns correspond to the second couple of indices. The reference isotropic model is given by

$$v_{\mathrm{P}}^2 = 15.00\,\mathrm{km}^2\mathrm{s}^{-2} \quad , \qquad v_{\mathrm{S}}^2 = 5.10\,\mathrm{km}^2\mathrm{s}^{-2} \tag{59}$$

at the surface, and

$$v_{\mathrm{P}}^2 = 23.00\,\mathrm{km}^2\mathrm{s}^{-2} \quad , \qquad v_{\mathrm{S}}^2 = 7.79\,\mathrm{km}^2\mathrm{s}^{-2} \tag{60}$$

at the depth of 1 km. All the above values are interpolated linearly with depth. The density is constant.

The synthetic seismograms, corresponding to vertical force $\mathbf{F} = (0, 0, 100)^{\mathrm{T}}$ at position $(50, 50, 0)^{\mathrm{T}}$, are calculated at 29 receivers $(51, 50, 0.010)^{\mathrm{T}}$, $(51, 50, 0.030)^{\mathrm{T}}$, $(51, 50, 0.050)^{\mathrm{T}}$, ..., $(51, 50, 0.570)^{\mathrm{T}}$ located in a vertical well (distances in km). The source time function is the Gabor signal $\cos(2\pi f t)\exp[-(2\pi f t/4)^2]$ with reference frequency $f = 50$ Hz, band–pass filtered by a cosine filter given by frequencies 0 Hz, 5 Hz, 60 Hz and 100 Hz.

The data for model QI may be found on the compact disk of *Bucha and Bulant (2002)* together with the Fortran 77 source code of packages CRT (*Červený, Klimeš and Pšenčík, 1988*) and ANRAY (*Gajewski and Pšenčík, 1990*; *Pšenčík, 1998b*). For comparison with the isotropic–ray–theory and anisotropic–ray–theory seismograms in model QI and for a more detailed discussion and description of this model refer to *Pšenčík and Dellinger (2001)*.

3.2. Models QI2, QI4 and QI8

To emphasize the effects of perturbations of travel time, new models with an increased degree of anisotropy have been derived from the QI model.

The differences of the elastic moduli of model QI2 from the elastic moduli of the reference isotropic model (59), (60) are exactly twice larger than the differences of model QI. The density–normalized elastic moduli a_{ijkl} of model QI2 in $\mathrm{km}^2\mathrm{s}^{-2}$ at the surface (zero depth) are

$$\begin{array}{c} \\ 11 \\ 22 \\ 33 \\ 23 \\ 13 \\ 12 \end{array}
\begin{array}{c}
\begin{array}{cccccc} 11 & 22 & 33 & 23 & 13 & 12 \end{array} \\
\begin{pmatrix}
13.97000 & 4.25000 & 4.70000 & 0.00000 & 0.00000 & -1.16000 \\
 & 13.97000 & 4.70000 & 0.00000 & 0.00000 & -1.16000 \\
 & & 16.42000 & 0.00000 & 0.00000 & -0.58000 \\
 & & & 5.21000 & -0.35000 & 0.00000 \\
 & & & & 5.21000 & 0.00000 \\
 & & & & & 4.99000
\end{pmatrix}
\end{array} \quad , \tag{61}$$

and at the depth of 1 km they are

$$\begin{array}{c} \\ 11 \\ 22 \\ 33 \\ 23 \\ 13 \\ 12 \end{array}
\begin{array}{c}
\begin{array}{cccccc} 11 & 22 & 33 & 23 & 13 & 12 \end{array} \\
\begin{pmatrix}
21.17926 & 6.38126 & 7.06750 & 0.00000 & 0.00000 & -1.76900 \\
 & 21.17926 & 7.06750 & 0.00000 & 0.00000 & -1.76900 \\
 & & 24.91550 & 0.00000 & 0.00000 & -0.88450 \\
 & & & 7.93276 & -0.53376 & 0.00000 \\
 & & & & 7.93276 & 0.00000 \\
 & & & & & 7.59726
\end{pmatrix}
\end{array} \quad . \tag{62}$$

Analogously, the differences of the elastic moduli of model QI4 from the elastic moduli of the reference isotropic model (59), (60) are exactly 4 times larger than the differences of model QI. The density–normalized elastic moduli a_{ijkl} of model QI4 in $\mathrm{km}^2\mathrm{s}^{-2}$ at the surface (zero depth) are

$$\begin{array}{c} \\ 11 \\ 22 \\ 33 \\ 23 \\ 13 \\ 12 \end{array}\begin{array}{c} \begin{array}{cccccc} \quad 11 \quad & \quad 22 \quad & \quad 33 \quad & \quad 23 \quad & \quad 13 \quad & \quad 12 \quad \end{array} \\ \begin{pmatrix} 12.94000 & 3.70000 & 4.60000 & 0.00000 & 0.00000 & -2.32000 \\ & 12.94000 & 4.60000 & 0.00000 & 0.00000 & -2.32000 \\ & & 17.84000 & 0.00000 & 0.00000 & -1.16000 \\ & & & 5.32000 & -0.70000 & 0.00000 \\ & & & & 5.32000 & 0.00000 \\ & & & & & 4.88000 \end{pmatrix} \end{array} , \tag{63}$$

and at the depth of 1 km they are

$$\begin{array}{c} \\ 11 \\ 22 \\ 33 \\ 23 \\ 13 \\ 12 \end{array}\begin{array}{c} \begin{array}{cccccc} \quad 11 \quad & \quad 22 \quad & \quad 33 \quad & \quad 23 \quad & \quad 13 \quad & \quad 12 \quad \end{array} \\ \begin{pmatrix} 19.35852 & 5.34252 & 6.71500 & 0.00000 & 0.00000 & -3.53800 \\ & 19.35852 & 6.71500 & 0.00000 & 0.00000 & -3.53800 \\ & & 26.83100 & 0.00000 & 0.00000 & -1.76900 \\ & & & 8.07552 & -1.06752 & 0.00000 \\ & & & & 8.07552 & 0.00000 \\ & & & & & 7.40452 \end{pmatrix} \end{array} . \tag{64}$$

Note that the perturbation approach cannot be applied to model QI8, in which the differences of the elastic moduli from the elastic moduli of the reference isotropic model (59), (60) are exactly 8 times larger than the differences of model QI. Perturbation expansion (17) does not seem to converge reasonably in model QI8.

The data for models QI2, QI4 and QI8 have been released on the compact disk of *Bucha and Bulant (2002)*. Numerical examples in this paper have been calculated using the data by *Bucha and Bulant (2002)*, with slightly refined parameters for isotropic two–point ray tracing.

3.3. Effects of quasi–isotropic approximations of reference rays

Two–point isotropic common rays have been traced from the source to the receivers using the program CRT, and the first–order and second–order perturbation derivatives of travel time have been calculated along these rays. Equations (18) and (19) have then been used to estimate both the travel–time errors $\delta\tau_1^{\mathrm{ICR}}$, $\delta\tau_2^{\mathrm{ICR}}$ of the isotropic common ray approximation and the travel–time errors $\delta\tau_1^{\mathrm{ACR}} = \delta\tau_2^{\mathrm{ACR}}$ of the anisotropic common ray approximation. The projection of the travel–time errors $\delta\tau_\alpha^{\mathrm{ICR}}$ on the relative error of the coupled S wavefield depends on the polarization. For the projection of the travel–time errors on the relative errors of the time–harmonic Green tensor refer to Section 3.5. To check the convergency and accuracy of the second–order perturbation expansion (17) of the anisotropic–ray–theory travel times, the perturbation expansion has been compared with the anisotropic–ray–theory travel times calculated by the program ANRAY along two–point anisotropic–ray–theory rays.

The individual terms in the second–order perturbation expansion (17) of both the anisotropic–ray–theory travel times are displayed in Tables 1, 2 and 3, for models QI, QI2 and QI4, respectively. The differences between the second–order perturbation expansion (17) and the anisotropic–ray–theory travel times calculated by the program ANRAY are also given. The quadratic terms (18) in perturbation expansion (17) represent the estimates of the errors due to the isotropic common ray (ICR) approximation of the anisotropic–ray–theory travel times. Also shown is the estimate (19) of the errors due to the anisotropic common ray (ACR) approximation. Only the results at the 1$^{\mathrm{st}}$, 8$^{\mathrm{th}}$, 15$^{\mathrm{th}}$, 22$^{\mathrm{nd}}$ and 29$^{\mathrm{th}}$ receivers are shown, because the variation of the quantities along the vertical profile in models QI, QI2 and QI4 is very moderate.

Since we are currently not able to solve the coupling equation along the anisotropic–ray–theory reference rays, we simulated the corresponding coupling–ray–theory synthetic seismograms by solving the coupling equations along isotropic common rays, with anisotropic–ray–theory travel times approximated by the second–order perturbation expansion (17). According to Tables 1, 2 and 3, the accuracy of the simulation should be sufficient for graphical demonstration of the effect of the isotropic common ray approximation on the coupling–ray–theory synthetic seismograms. The simulated seismograms of the coupling ray theory in model QI are compared with the seismograms calculated by the isotropic common ray approximation in Figure 1. The alteration of the seismograms due to the isotropic common ray approximation is scarcely visible in model QI. To make the alteration of the seismograms due to the isotropic common ray approximation more visible, an analogous comparison, but in model QI2, is shown in Figure 3. The first–order isotropic common ray approximation is considerably inaccurate in model QI4, see the seismograms of Figure 5.

Although we have successfully applied the second–order perturbation expansion of travel time to the estimation of anisotropic–ray–theory travel times in these simple 1-D models with constant gradients of the density–normalized elastic moduli, we cannot recommend approximation of travel time using the second–order perturbation expansion in more complex models, because the second–order perturbation derivatives may be infinitely large in the vicinity of caustics. The second–order perturbation expansion of travel time should be used especially for estimating and controlling the accuracy.

The maximum travel–time error of 0.000253 seconds of the isotropic common ray approximation in model QI corresponds to the wavefield relative error of 7.9% at 50 Hz.

The maximum travel–time error of 0.000978 seconds of the isotropic common ray approximation in model QI2 is clearly visible in Figure 3, and corresponds to the wavefield relative error of 31% at 50 Hz. The accuracy of the anisotropic common ray approximation by *Bakker (2002)* in model QI2 would be even better than the accuracy of the isotropic common ray approximation in model QI, see Tables 1 and 2.

Table 1. Linear and quadratic terms in the common ray approximations of travel time in model QI.

Rec. dep.	ICR time	ICR linear terms		ICR quadratic terms		ICR remaining terms		ACR q.terms
0.01	0.440993	-0.002392	0.003983	0.000253	0.000000	-0.000003	-0.000001	0.000066
0.15	0.438077	-0.002518	0.004003	0.000250	0.000000	0.000007	-0.000001	0.000066
0.29	0.443550	-0.002967	0.004117	0.000251	0.000001	0.000007	0.000001	0.000069
0.43	0.456339	-0.003661	0.004317	0.000253	0.000001	0.000008	-0.000002	0.000073
0.57	0.475205	-0.004520	0.004595	0.000251	0.000003	0.000020	0.000006	0.000076

Table 2. Linear and quadratic terms in the common ray approximations of travel time in model QI2.

Rec. dep.	ICR time	ICR linear terms		ICR quadratic terms		ICR remaining terms		ACR q.terms
0.01	0.440993	-0.004746	0.011604	0.000978	0.000000	0.000001	-0.000007	0.000237
0.15	0.438077	-0.004992	0.011612	0.000967	0.000000	0.000015	0.000001	0.000233
0.29	0.443550	-0.005874	0.011837	0.000967	0.000001	0.000029	0.000005	0.000230
0.43	0.456339	-0.007234	0.012235	0.000965	0.000001	0.000047	0.000001	0.000226
0.57	0.475205	-0.008912	0.012764	0.000951	0.000002	0.000063	0.000000	0.000218

Table 3. Linear and quadratic terms in the common ray approximations of travel time in model QI4.

Rec. dep.	ICR time	ICR linear terms		ICR quadratic terms		ICR remaining terms		ACR q.terms
0.01	0.440993	-0.009341	0.041580	0.003671	0.000492	0.000092	-0.000141	0.000367
0.15	0.438077	-0.009816	0.041343	0.003616	0.000553	0.000137	-0.000147	0.000335
0.29	0.443550	-0.011517	0.041462	0.003580	0.000718	0.000224	-0.000174	0.000273
0.43	0.456339	-0.014129	0.041796	0.003520	0.000962	0.000328	-0.000212	0.000201
0.57	0.475205	-0.017335	0.042243	0.003415	0.001234	0.000434	-0.000234	0.000136

Tables 1, 2 and 3. *Rec. dep.* stands for the receiver depth along the vertical profile, see Figures 1 to 6. The *ICR time* is the reference travel time τ along the isotropic common ray. The *ICR linear terms* are the linear terms $\tau_{,1}$ and $\tau_{,2}$ in perturbation expansion (17) of the anisotropic–ray–theory travel times in the vicinity of the isotropic common ray, and represent the travel–time corrections considered in the isotropic common ray approximation of the coupling ray theory. The *ICR quadratic terms* stand for quadratic terms (18) in perturbation expansion (17) of travel time, and represent the estimates of the errors due to the isotropic common ray approximation of the anisotropic–ray–theory travel times. The *ICR remaining terms* stand for the difference between the exact anisotropic–ray–theory travel times calculated by the program ANRAY version 4.40 (*Gajewski and Pšenčík, 1990*; *Pšenčík, 1998b*) and the second–order perturbation expansion (17), in order to illustrate the reliability of the error estimates. The ICR remaining terms represent both the inaccuracy of numerical ray tracing and the third–order and higher–order terms in the perturbation expansion. The *ACR quadratic terms* stand for the estimate (19) of the equal quadratic terms in the perturbation expansion of the anisotropic–ray–theory travel times in the vicinity of the anisotropic common ray, and represent the estimate of the error due to the anisotropic common ray approximation (*Bakker, 2002*) of the anisotropic–ray–theory travel times.

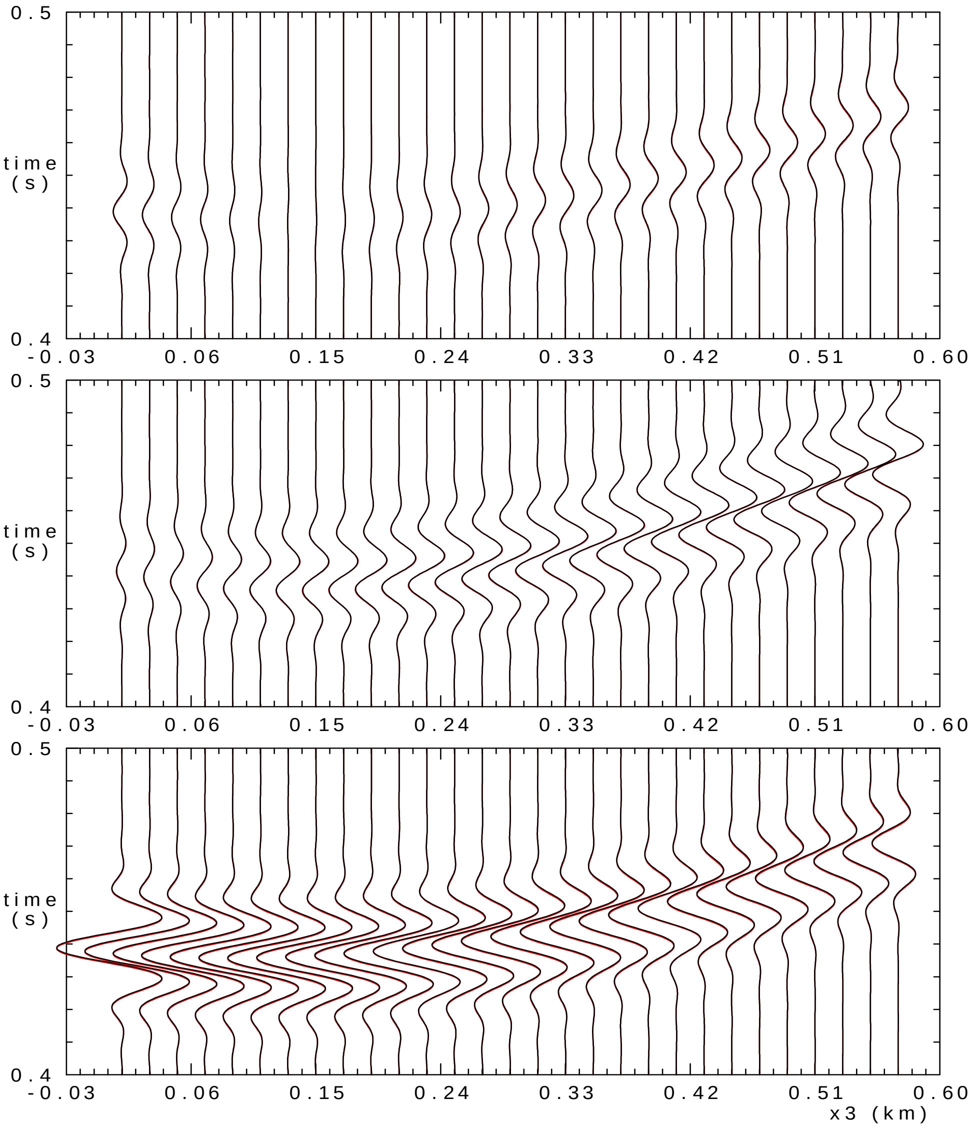

Fig. 1. Effect of the isotropic common ray approximation on the coupling–ray–theory synthetic seismograms in model QI. From top to bottom: the first (radial) component, the second (transverse) component, the third (vertical) component. Note that the second component is zero in the one–dimensional reference isotropic model. **Black:** No quasi–isotropic approximation. These seismograms are simulated by the second–order perturbation expansion of travel time along isotropic common rays, rather than calculated along the anisotropic–ray–theory reference rays. The inaccuracy of this simulation cannot be seen, see Table 1. **Red:** Isotropic common ray approximation. The red seismograms are mostly obscured by the black seismograms.

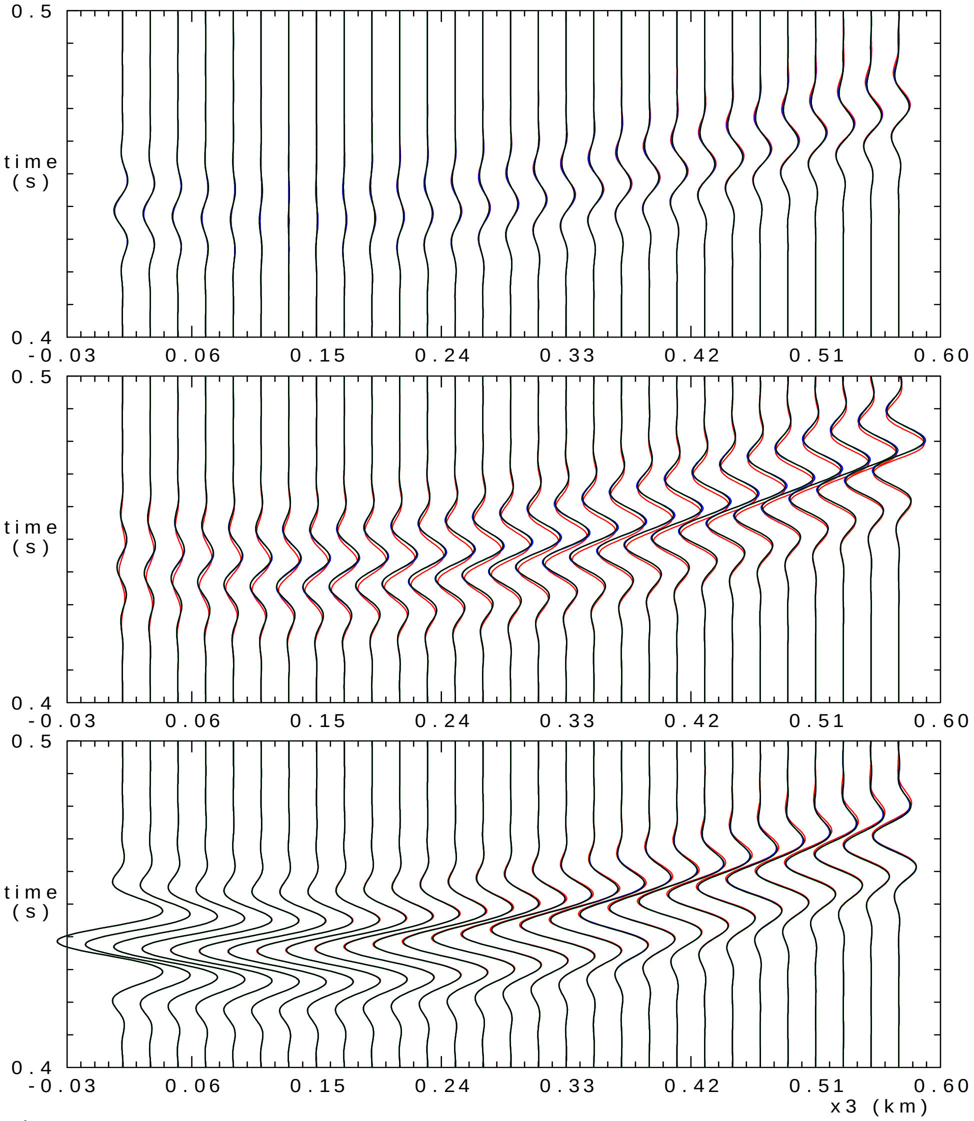

Fig. 2. Effects of the other three quasi–isotropic approximations on the coupling–ray–theory synthetic seismograms in model QI. From top to bottom: the first (radial) component, the second (transverse) component, the third (vertical) component. The isotropic common ray approximation is applied to all synthetic seismograms. **Black:** No additional quasi–isotropic approximation. **Blue:** Quasi–isotropic projection of the Green tensor. The blue seismograms are mostly obscured by the black seismograms. A small change in polarization can be seen in the second (transverse) component. **Red:** Quasi–isotropic approximation of the Christoffel matrix. Note that this impact of the quasi–isotropic approximation of the Christoffel matrix on the coupling–ray–theory synthetic seismograms in model QI, clearly visible in the second (transverse) component, has already been demonstrated by *Bulant and Klimeš (2002)*. **Green:** Quasi–isotropic perturbation of travel times. Negligible impact in model QI, the green seismograms are obscured by the black seismograms.

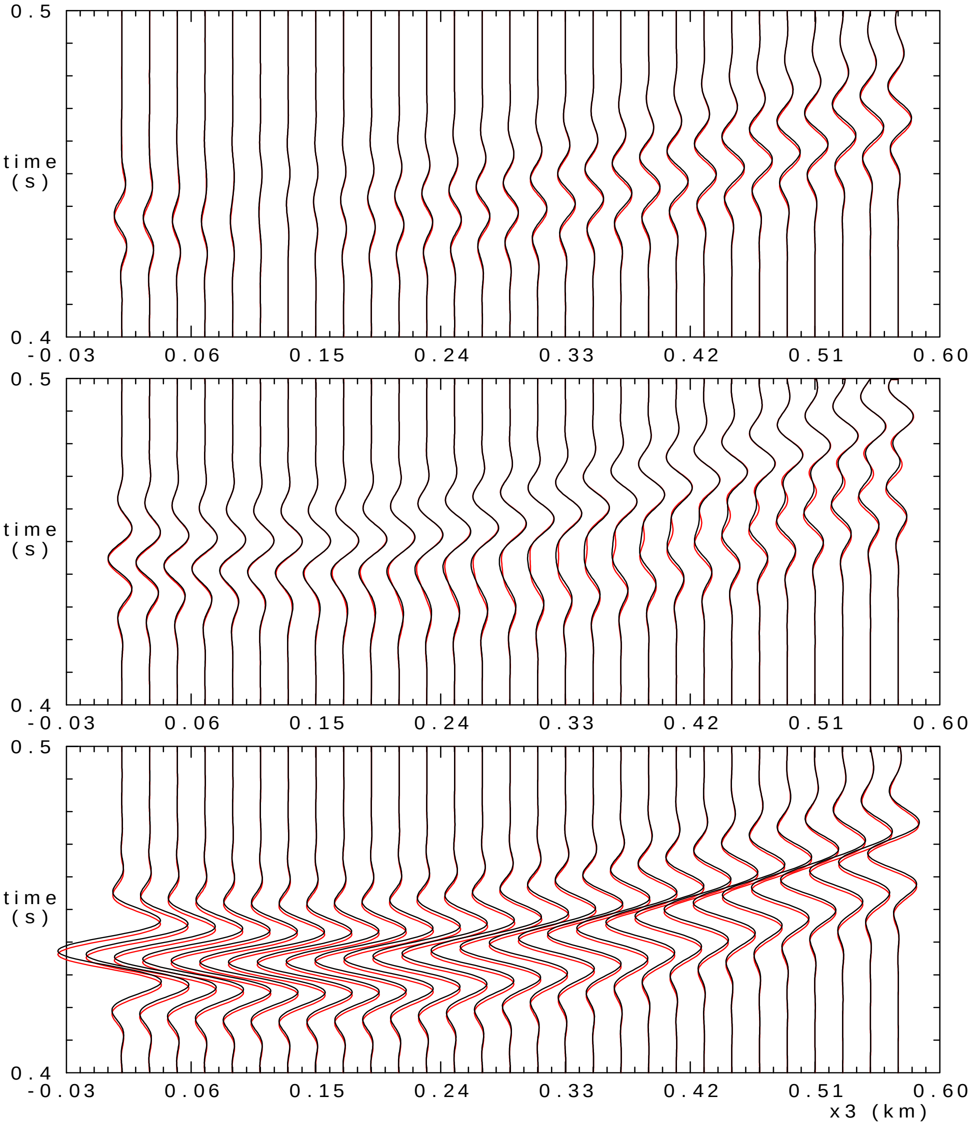

Fig. 3. Effect of the isotropic common ray approximation on the coupling–ray–theory synthetic seismograms in model QI2. From top to bottom: the first (radial) component, the second (transverse) component, the third (vertical) component. **Black:** No quasi–isotropic approximation. These seismograms are simulated by the second–order perturbation expansion of travel time along isotropic common rays, rather than calculated along the anisotropic–ray–theory reference rays. The inaccuracy of this simulation cannot be seen, see Table 2. **Red:** Isotropic common ray approximation. The differences between the seismograms are small but already clearly visible.

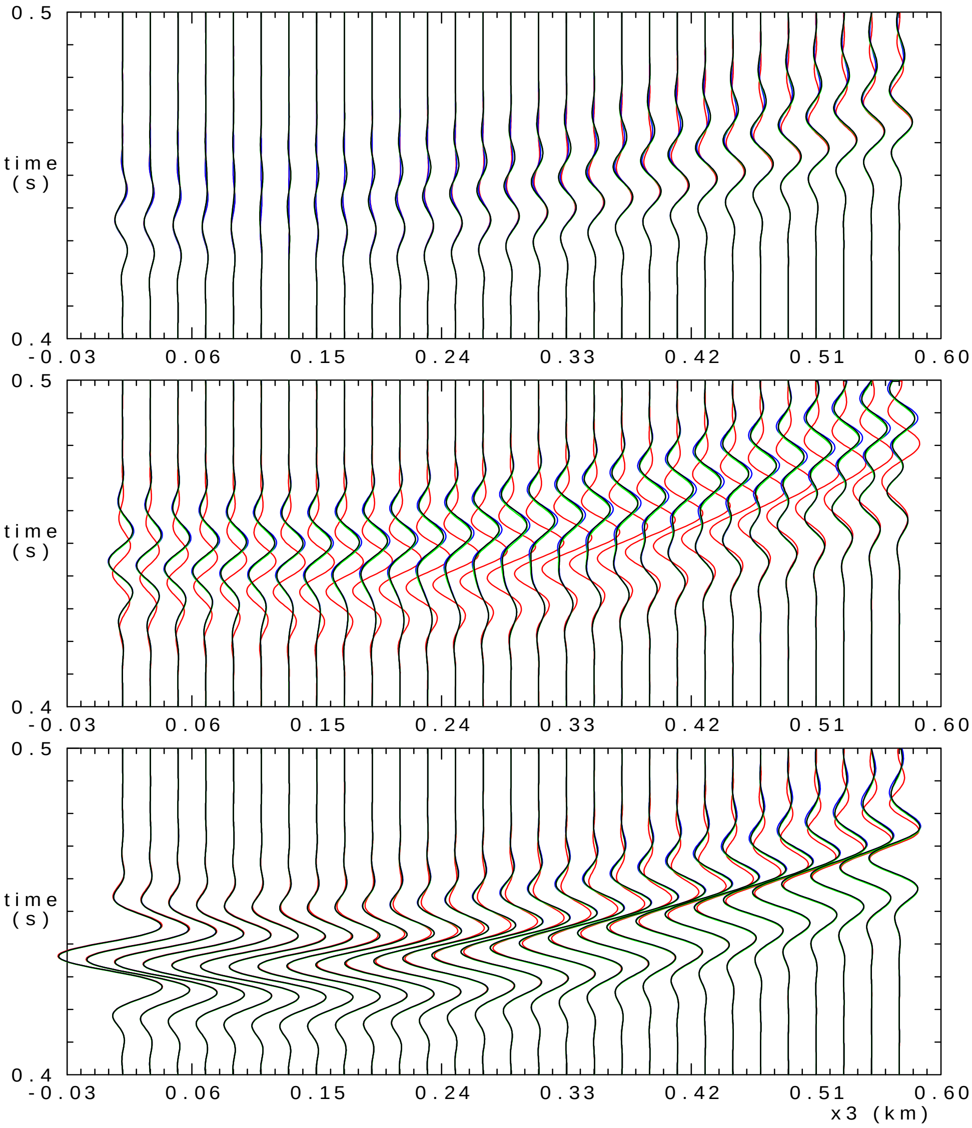

Fig. 4. Effects of the other three quasi–isotropic approximations on the coupling–ray–theory synthetic seismograms in model QI2. From top to bottom: the first (radial) component, the second (transverse) component, the third (vertical) component. The isotropic common ray approximation is applied to all synthetic seismograms. **Black:** No additional quasi–isotropic approximation. **Blue:** Quasi–isotropic projection of the Green tensor. Clearly visible in the second (transverse) component, otherwise mostly obscured by the black seismograms. **Red:** Quasi–isotropic approximation of the Christoffel matrix. **Green:** Quasi–isotropic perturbation of travel times. Partly obscured by the black seismograms.

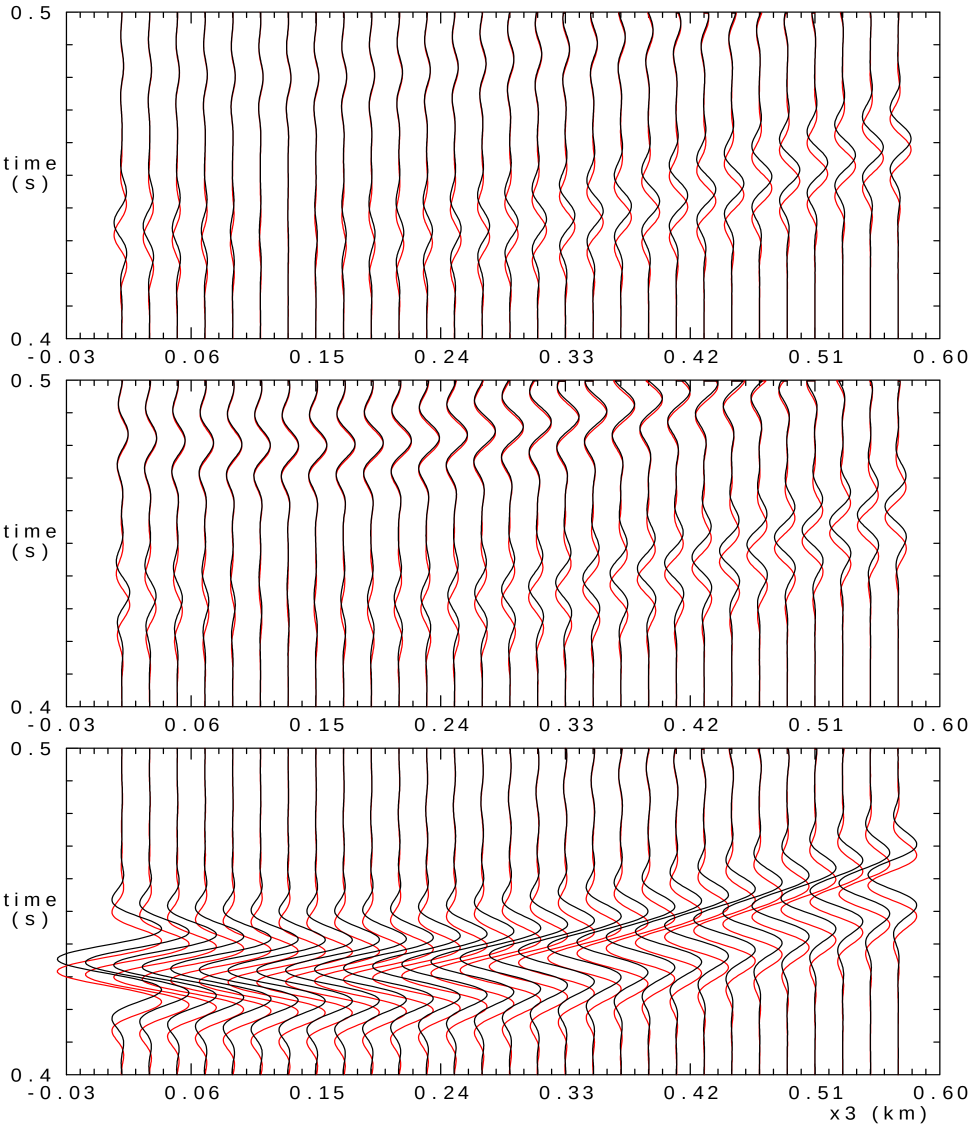

Fig. 5. Effect of the isotropic common ray approximation on the coupling–ray–theory synthetic seismograms in model QI4. From top to bottom: the first (radial) component, the second (transverse) component, the third (vertical) component. **Black:** No quasi–isotropic approximation. These seismograms are simulated by the second–order perturbation expansion of travel time along isotropic common rays, rather than calculated along the anisotropic–ray–theory reference rays. The inaccuracy of this simulation in model QI4 roughly corresponds to the line thickness, see Table 3. **Red:** Isotropic common ray approximation. The differences between the seismograms are considerable in this quite strongly anisotropic model QI4.

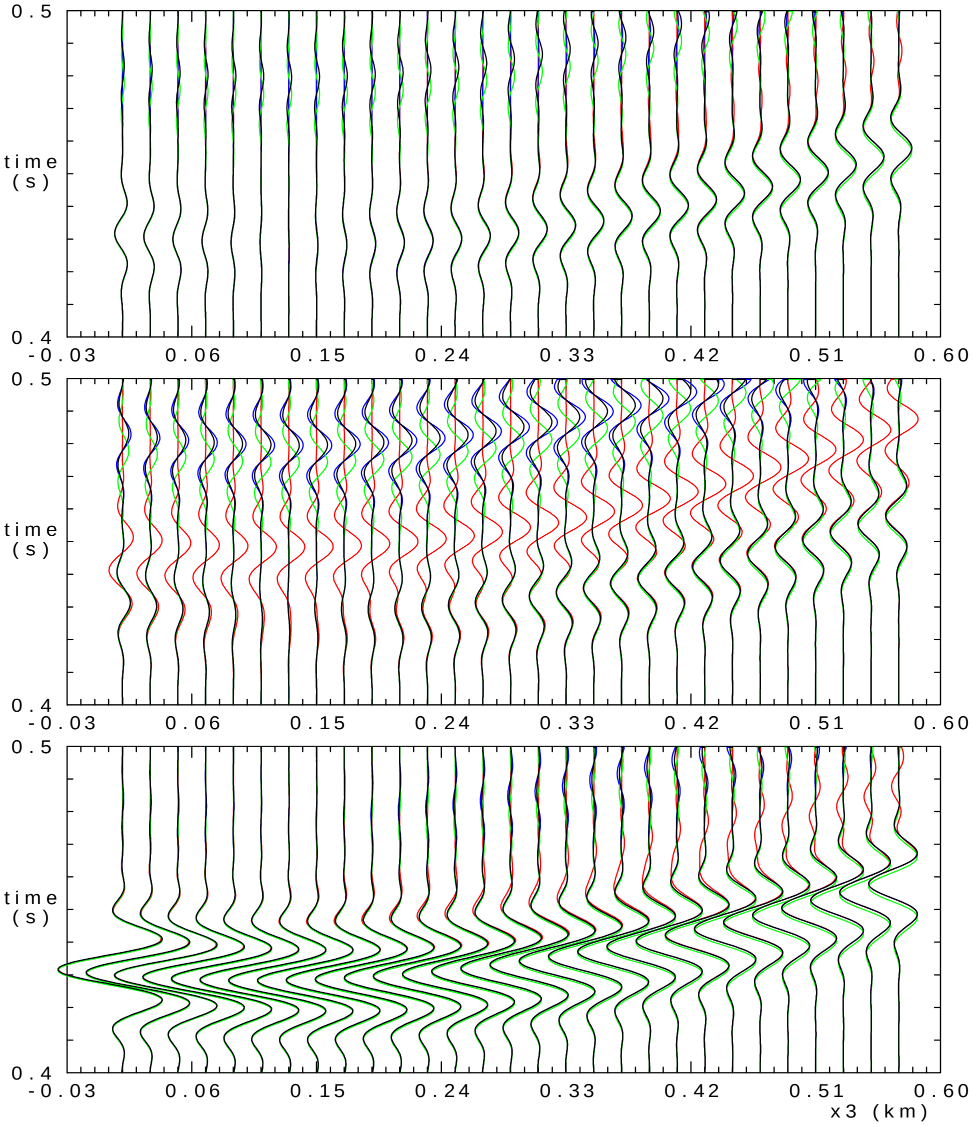

Fig. 6. Effects of the other three quasi–isotropic approximations on the coupling–ray–theory synthetic seismograms in model QI4. From top to bottom: the first (radial) component, the second (transverse) component, the third (vertical) component. The isotropic common ray approximation is applied to all synthetic seismograms. **Black:** No additional quasi–isotropic approximation. **Blue:** Quasi–isotropic projection of the Green tensor. Clearly visible on the slower S wave, otherwise obscured by the black seismograms. **Red:** Quasi–isotropic approximation of the Christoffel matrix. This approximation slightly turns the polarization of the slower S wave towards the P–wave polarization (see blue seismograms), and in this way strongly affects the phase velocity of the slower S wave along the reference ray. **Green:** Quasi–isotropic perturbation of travel times.

The first–order isotropic common ray approximation is considerably inaccurate in model QI4, see Figure 5 and Table 3. The inaccuracy of the second–order perturbation expansion (17) of travel time in model QI4 roughly corresponds to the line thickness in Figure 5. The first–order anisotropic common ray approximation by *Bakker (2002)* seems well applicable even in this quite strongly anisotropic model QI4, and its accuracy is even better than the accuracy of the second–order perturbation expansion (17) from the isotropic common ray, see Table 3.

3.4. Comparison with the effects of other quasi–isotropic approximations

We now numerically compare the error due to the *isotropic common ray* (ICR) *approximation* with the errors due to the quasi–isotropic projection of the Green tensor, due to the quasi–isotropic approximation of the Christoffel matrix, and due to the quasi–isotropic perturbation of travel times. The impact of these three quasi–isotropic approximations on the coupling–ray–theory synthetic seismograms in models QI, QI2 and QI4 is demonstrated in Figures 2, 4 and 6, respectively.

In the *quasi–isotropic projection of the Green tensor* (*Bulant and Klimeš, 2002,* appendix A.2*; 2004,* sec. 3.2), the S–wave coupling–ray–theory Green tensor is projected onto the reference polarization planes perpendicular to the reference ray. The projection is applied at the source and receiver points. The relative wavefield error due to the projection is frequency–independent and is roughly proportional to the degree of anisotropy.

In the *quasi–isotropic approximation of the Christoffel matrix* (*Bulant and Klimeš, 2002,* appendix A.3*; 2004,* sec. 3.3), the Christoffel matrix is approximated by its projections onto the reference S–wave polarization plane perpendicular to the reference ray and onto the reference P–wave polarization line tangent to the reference ray. The projection is applied along the reference ray and distorts the S–wave travel times towards the P–wave travel time. The relative wavefield error due to this approximation is proportional to frequency and is roughly proportional to the square of the degree of anisotropy. The impact of the quasi–isotropic approximation of the Christoffel matrix on the coupling–ray–theory synthetic seismograms has already been demonstrated in model QI by *Bulant and Klimeš (2002)* using the data from the compact disk of *Bucha, Bulant and Klimeš (2001).*

In the *quasi–isotropic perturbation of travel times* (*Bulant and Klimeš, 2002,* appendix A.4*; 2004,* sec. 3.4), the anisotropic–ray–theory travel times are approximated by the first–order perturbation expansion with respect to the density–normalized elastic moduli, instead of using the more accurate travel–time approximation (2). The quasi–isotropic perturbation of travel times corresponds to substituting Hamiltonian $H = -G^{-\frac{1}{2}}$, see (3), by Hamiltonian $H = \frac{1}{2}G$ (*Klimeš, 2002*). The relative wavefield error due to this approximation is proportional to frequency and is very roughly proportional to the square of the difference between the anisotropic model and the reference isotropic model, see equation (69) below.

3.5. Relative errors of the time–harmonic Green tensor due to the quasi–isotropic approximations

We define the relative root–mean–square (r.m.s.) difference between the time–harmonic Green tensors $G_{ij}^{(1)}$ and $G_{ij}^{(2)}$ as

$$\rho G = \sqrt{\frac{2\big(G_{ij}^{(1)} - G_{ij}^{(2)}\big)^{*}\,\big(G_{ij}^{(1)} - G_{ij}^{(2)}\big)}{\big(G_{mn}^{(1)}\big)^{*} G_{mn}^{(1)} + \big(G_{mn}^{(2)}\big)^{*} G_{mn}^{(2)}}} \quad , \tag{65}$$

where * denotes complex conjugacy. Component G_{ij} of the time–harmonic Green tensor between the source and receiver points represents the $i^{\rm th}$ component of the displacement at the receiver point caused by the unit time–harmonic seismic force applied in the direction of the $j^{\rm th}$ coordinate axis at the source point. Here we consider only the S–wave part of the Green tensor.

The relative r.m.s. error of the time–harmonic Green tensor at frequency f due to the isotropic common ray approximation can be estimated using travel–time errors (18). A rough approximation is

$$\rho G = 2\,\pi\, f\, \delta\tau^{\rm ICR} \quad , \tag{66}$$

where

$$\delta\tau^{\rm ICR} = \sqrt{\frac{(\delta\tau_1^{\rm ICR})^2 + (\delta\tau_2^{\rm ICR})^2}{2}} \tag{67}$$

is the r.m.s. travel–time error of the isotropic common ray approximation. Travel–time errors $\delta\tau_\alpha^{\rm ICR}$ of the isotropic common ray approximation, given by equation (18), are labelled as the *ICR quadratic terms* in Tables 1, 2 and 3. Note that a more precise estimate is

$$\rho G = \sqrt{2\{\,[\sin(\pi f \delta\tau_1^{\rm ICR})]^2 + [\sin(\pi f \delta\tau_2^{\rm ICR})]^2\}} \quad . \tag{68}$$

However, the difference between estimates (66) and (68) is negligible if the relative error is not extremely large. Even if the relative error (68) reaches 50%, estimate (66) yields 51%.

The relative r.m.s. error of the time–harmonic Green tensor due to the quasi–isotropic perturbation of travel times may roughly be approximated by the undervalued estimate

$$\rho G = 3\,\pi\, f\, \frac{(\tau_{,1})^2 + (\tau_{,2})^2}{2\,\tau} \quad , \tag{69}$$

where $\tau_{,\alpha}$ are the first–order perturbation derivatives in perturbation expansion (17), labelled as *ICR linear terms* in Tables 1, 2 and 3.

The relative r.m.s. errors of the time–harmonic Green tensor at frequency $f =$ 50 Hz due to the four quasi–isotropic approximations of the coupling ray theory are compared in Tables 4, 5 and 6. The error due to the isotropic common ray approximation is also compared with its estimates (66) and (68). The error due to the quasi–isotropic perturbation of travel times is compared with its estimate (69).

Table 4. Relative r.m.s. error of the time–harmonic Green tensor at 50 Hz due to various quasi–isotropic approximations in model QI.

Receiver depth	ICR eq. (66)	ICR eq. (68)	ICR numeric	QI project. Green t.	QI appr. Christ.m.	QI travel times	QI t.t. eq. (69)
0.01	0.056	0.056	0.056	0.061	0.348	0.013	0.012
0.15	0.056	0.056	0.055	0.061	0.346	0.013	0.012
0.29	0.056	0.056	0.056	0.061	0.350	0.014	0.014
0.43	0.056	0.056	0.056	0.060	0.355	0.017	0.017
0.57	0.056	0.056	0.056	0.058	0.358	0.021	0.021

Table 5. Relative r.m.s. error of the time–harmonic Green tensor at 50 Hz due to various quasi–isotropic approximations in model QI2.

Receiver depth	ICR eq. (66)	ICR eq. (68)	ICR numeric	QI project. Green t.	QI appr. Christ.m.	QI travel times	QI t.t. eq. (69)
0.01	0.217	0.216	0.216	0.126	1.227	0.100	0.084
0.15	0.215	0.214	0.214	0.125	1.221	0.101	0.086
0.29	0.215	0.214	0.214	0.124	1.225	0.105	0.093
0.43	0.214	0.214	0.213	0.121	1.230	0.113	0.104
0.57	0.211	0.210	0.211	0.117	1.230	0.124	0.120

Table 6. Relative r.m.s. error of the time–harmonic Green tensor at 50 Hz due to various quasi–isotropic approximations in model QI4.

Receiver depth	ICR eq. (66)	ICR eq. (68)	ICR numeric	QI project. Green t.	QI appr. Christ.m.	QI travel times	QI t.t. eq. (69)
0.01	0.823	0.779	0.779	0.256	N/A	1.036	0.970
0.15	0.813	0.771	0.771	0.255	N/A	1.033	0.971
0.29	0.811	0.771	0.771	0.249	N/A	1.031	0.984
0.43	0.811	0.773	0.773	0.241	N/A	1.030	1.005
0.57	0.807	0.773	0.773	0.230	N/A	1.031	1.034

Tables 4, 5 and 6. The *receiver depth* is measured along the vertical profile, see Figures 1 to 6. *ICR eq.* (66) stands for the relative r.m.s. error of the Green tensor due to the isotropic common ray approximation, estimated from the r.m.s. error of travel times using equation (66). *ICR eq.* (68) stands for the relative r.m.s. error of the Green tensor due to the isotropic common ray approximation, estimated from the r.m.s. error of travel times using equation (68). *ICR numeric* is the actual relative r.m.s. error of the Green tensor due to the isotropic common ray approximation. The *QI project. Green t.* is the relative r.m.s. error of the Green tensor due to the quasi–isotropic projection of the Green tensor. The *QI appr. Christ.m.* means the relative r.m.s. error of the Green tensor due to the quasi–isotropic approximation of the Christoffel matrix. Label *QI travel times* denotes the actual relative r.m.s. error of the Green tensor due to the quasi–isotropic perturbation of travel times. *QI t.t. eq.* (69) stands for estimate (69) of the relative r.m.s. error of the Green tensor due to the quasi–isotropic perturbation of travel times.

4. CONCLUSIONS

In using any kind of common ray approximation of the coupling ray theory, the travel–time errors due to the applied common ray approximation should be evaluated. The travel–time errors due to the common ray approximations can be calculated using the equations proposed in this paper. If the error of the isotropic common ray approximation exceeds an acceptable limit, we can immediately decide whether the anisotropic common ray approximation (*Bakker, 2002*; *Klimeš, 2003*) would be sufficiently accurate, or whether the anisotropic–ray–theory rays should be traced as reference rays for the coupling ray theory. The accuracy of the anisotropic common ray approximation by *Bakker (2002)* can be studied without tracing the anisotropic common rays. The numerical results suggest that the anisotropic common ray approximation by *Bakker (2002)* is worth coding and applying.

The quasi–isotropic projection of the Green tensor, the quasi–isotropic approximation of the Christoffel matrix, and the quasi–isotropic perturbation of travel times should definitely be avoided.

For additional information, including electronic reprints, computer codes and data, refer to the consortium research project "Seismic Waves in Complex 3-D Structures" ("http://sw3d.mff.cuni.cz").

Acknowledgements: The authors are grateful to Ivan Pšenčík and two anonymous reviewers whose comments enabled the improvement of this paper.

The research has been supported by the Grant Agency of the Czech Republic under Contracts 205/01/0927, 205/01/D097 and 205/04/1104, by the Grant Agency of the Charles University under Contracts 237/2001/B-GEO/MFF and 229/2002/B-GEO/MFF, by the Ministry of Education of the Czech Republic within Research Project MSM113200004, and by the members of the consortium "Seismic Waves in Complex 3-D Structures" (see "http://sw3d.mff.cuni.cz").

References

Arnaud, J.A., 1973. Hamiltonian theory of beam mode propagation. In: Wolf, E. (ed.): *Progress in Optics, Vol. 11*, pp. 247–304, North–Holland, Amsterdam–London.

Babich, V.M. and Buldyrev, N.J., 1972. *Asymptotic Methods in Problems of Diffraction of Short Waves.* Nauka, Moscow (in Russian).

Bakker, P.M., 2002. Coupled anisotropic shear wave raytracing in situations where associated slowness sheets are almost tangent. *Pure Appl. Geophys.*, **159**, 1403–1417.

Baumgärtel, H., 1985. *Analytic Perturbation Theory for Matrices and Operators.* Birkhäuser, Basel.

Bucha, V. and Bulant, P. (eds.), 2002. SW3D–CD–6 (CD–ROM). In: *Seismic Waves in Complex 3-D Structures, Report 12*, pp. 247–247, Dep. Geophys., Charles Univ., Prague, online at "http://sw3d.mff.cuni.cz".

Bucha, V., Bulant, P. and Klimeš, L. (eds.), 2001. SW3D–CD–5 (CD–ROM). In: *Seismic Waves in Complex 3-D Structures, Report 11*, pp. 357–357, Dep. Geophys., Charles Univ., Prague, online at "http://sw3d.mff.cuni.cz".

Bulant, P. and Klimeš, L., 2002. Numerical algorithm of the coupling ray theory in weakly anisotropic media. *Pure Appl. Geophys.*, **159**, 1419–1435.

Bulant, P. and Klimeš, L., 2004. Comparison of quasi–isotropic approximations of the coupling ray theory with the exact solution in the 1-D anisotropic "oblique twisted crystal" model. *Stud. Geophys. Geod.*, **48**, 97–116.

Červený, V., 1972. Seismic rays and ray intensities in inhomogeneous anisotropic media. *Geophys. J. R. Astr. Soc.*, **29**, 1–13.

Červený, V., 2001. *Seismic Ray Theory.* Cambridge Univ. Press, Cambridge.

Červený, V. and Hron, F., 1980. The ray series method and dynamic ray tracing system for three–dimensional inhomogeneous media. *Bull. Seismol. Soc. Am.*, **70**, 47–77.

Červený, V., Klimeš, L. and Pšenčík, I., 1988. Complete seismic–ray tracing in three–dimensional structures. In: Doornbos, D.J. (ed.): *Seismological Algorithms*, pp. 89–168, Academic Press, New York.

Coates, R.T. and Chapman, C.H., 1990. Quasi–shear wave coupling in weakly anisotropic 3-D media. *Geophys. J. Int.*, **103**, 301–320.

Gajewski, D. and Pšenčík, I., 1990. Vertical seismic profile synthetics by dynamic ray tracing in laterally varying layered anisotropic structures. *J. Geophys. Res.*, **95B**, 11301–11315.

Klimeš, L., 2002. Second–order and higher–order perturbations of travel time in isotropic and anisotropic media. *Stud. Geophys. Geod.*, **46**, 213–248.

Klimeš, L., 2003. Common ray tracing and dynamic ray tracing for S waves in a smooth elastic anisotropic medium. In: *Seismic Waves in Complex 3-D Structures, Report 13*, pp. 119–141, Dep. Geophys., Charles Univ., Prague, online at "http://sw3d.mff.cuni.cz".

Luneburg, R.K., 1944. *Mathematical Theory of Optics.* Lecture notes, Brown University, Providence, Rhode Island. Reedition: University of California Press, Berkeley and Los Angeles, 1964.

Popov, M.M. and Pšenčík, I., 1978a. Ray amplitudes in inhomogeneous media with curved interfaces. *Travaux Instit. Géophys. Acad. Tchécosl. Sci. No. 454, Geofys. Sborník*, **24**, 111–129, Academia, Praha.

Popov, M.M. and Pšenčík, I., 1978b. Computation of ray amplitudes in inhomogeneous media with curved interfaces. *Stud. Geophys. Geod.*, **22**, 248–258.

Pšenčík, I., 1998a. Green's functions for inhomogeneous weakly anisotropic media. *Geophys. J. Int.*, **135**, 279–288.

Pšenčík, I., 1998b. Package ANRAY, version 4.10. In: *Seismic Waves in Complex 3-D Structures, Report 7*, pp. 403–404, Dep. Geophys., Charles Univ., Prague, online at "http://sw3d.mff.cuni.cz".

Pšenčík, I. and Dellinger, J., 2001. Quasi–shear waves in inhomogeneous weakly anisotropic media by the quasi–isotropic approach: A model study. *Geophysics*, **66**, 308–319.

Tarantola, A., 1987. Inversion of travel times and seismic waveforms. In: Nolet, G. (ed.): *Sesmic Tomography*, pp. 135–157, D. Reidel Publ. Co., Dordrecht.

Vavryčuk, V., 2001. Ray tracing in anisotropic media with singularities. *Geophys. J. Int.*, **145**, 265–276.